Crystal Phase Quantum Dots

N. Akopian,*,† G. Patriarche,‡ L. Liu,† J.-C. Harmand,‡ and V. Zwiller†

†Kavli Institute of Nanoscience, Delft University of Technology, 2628CJ Delft, The Netherlands, and ‡Laboratoire de Photonique et de Nanostructures, CNRS, route de Nozay, 91460 Marcoussis, France

ABSTRACT In semiconducting nanowires, both zinc blende and wurtzite[1] crystal structures can coexist.[2−4] The band structure difference between the two structures can lead to charge confinement.[5] Here we fabricate and study single quantum dot devices[6] defined solely by crystal phase in a chemically homogeneous nanowire and observe single photon generation. More generally, our results show that this type of carrier confinement represents a novel degree of freedom in device design at the nanoscale.

KEYWORDS Nanowires, quantum dots, crystal phase, single photons, crystal structure

Nanowires (NWs) were grown for the first time in 1964 at Bell Laboratories by Wagner and Ellis.[7] These were individual silicon crystals with a diameter of about 100 nm and over 1.5 μm long. Three decades later, in 1991 Hiruma et al.[8] succeeded in growing the first III−V compound nanowires. A year later, the same group reported the existence of both zinc blende (ZB) and wurtzite (WZ) crystal structures in nanowires composed of a single material, indium arsenide in their case.[4] In 1994 calculations predicted band offsets at WZ−ZB interfaces.[5] However, the first successful attempts to control the phase of a crystal structure during nanowire growth[2,3] and the first optical studies[9−12] were reported only recently. This progress practically enables engineering of the electronic structure of a single material. For example, a superlattice of twin planes can induce a direct band gap in silicon[13] that would have a strong impact in semiconductor technology; a WZ−ZB−WZ heterointeface can define a quantum well in a single material. Growing such a structure in a nanowire will also confine charges in two other dimensions, forming a crystal phase quantum dot, which we demonstrate in this work.

The schematics of a crystal phase heterostructure is shown in Figure 1a. Our heterostructure is formed by growing indium phospide (InP) NW with two different crystal phases: wurtzite and zinc blende. Zinc blende has a smaller band gap and large negative band offset. Hence, the conduction and valence bands of zinc blende segments are lower in energy compared to wurtzite parts. Short zinc blende sections can confine electrons in the growth direction, and be barriers for holes. Two types of radiative recombinations are therefore possible. The first, labeled α, is the direct recombination of electron−hole pairs in the wurtzite part of a NW and, therefore, will result in a short lifetime. In the second transition, labeled β, electrons confined in zinc blende segments will recombine radiatively with holes in adjacent wurtzite regions of a NW. This spatially indirect electron−hole pair recombination will result in longer lifetimes, due to reduced overlap of electron and hole wave functions. Optical transitions of types α and β are represented in the photoluminescence (PL) schematics and correspond to emission peaks labeled as WZ and ZB/WZ respectively.

In addition, electrons (and holes) can be confined in two other dimensions, perpendicular to the growth direction, with a small enough NW diameter. The three-dimensional confinement will form a crystal phase quantum dot (QD) - it is formed from two different crystalline phases of the same material: wurtzite InP and zinc blende InP in our case, yielding quantized energy levels.[14] Their radiative recombination with holes in adjacent wurtzite parts of a NW will therefore be a source of singe photons.[15] The zinc blende segments lengths set the confined electrons energy levels. Accordingly, this will set energies and lifetimes of the emitted single photons.

Another case is when a short wurtzite segment is embedded between two short zinc blende segments: holes will be confined in a wurtzite segment and will be spatially separated from confined electrons. The indirect radiative recombination, labeled γ, will again result in longer lifetimes due to reduced overlap of electron and hole wave functions. Here, a crystal phase QD is formed for both electrons and holes.

In Figure 1b we show a transmission electron microscopy image of a single InP nanowire segment. Atomic planes of each crystal structure are colored: blue for wurtzite, red for zinc blende. Conversely to conventional heterostructures made of alternation of compounds, the crystal phase heterostructures have systematically an ideal interface with a steplike transition at the atomic scale.

Photoluminsecence spectra of a single InP nanowire at 4.2 K are shown in Figure 1c. The spectral line at 1.486 eV, labeled WZ, corresponds to electron−hole recombination of type α in the wurtzite part of the nanowire. All emission lines at lower energies, labeled ZB/WZ, correspond to electron−hole recombinations of type β or γ in crystal phase QDs. With
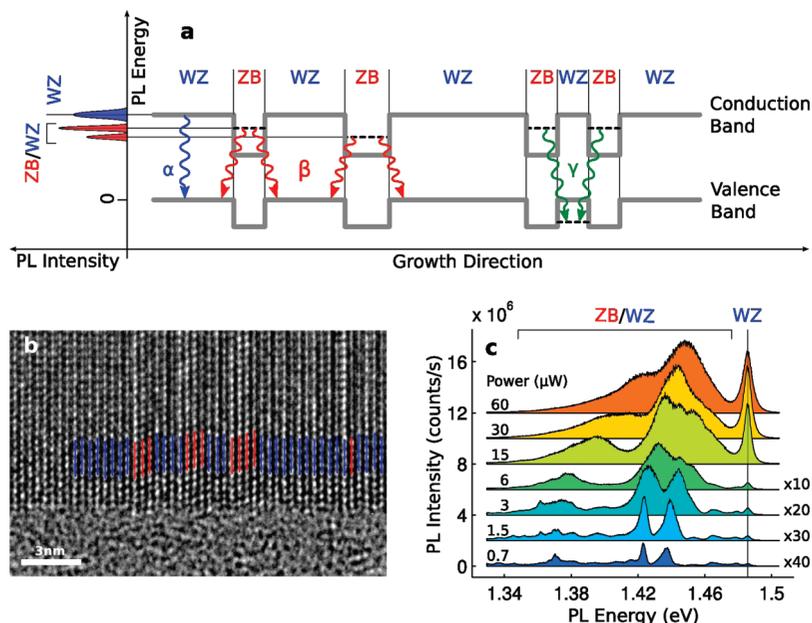
FIGURE 1. Crystal phase heterostructures. (a) Right: schematics of crystal phase heterostructures in an InP nanowire. Left: schematics of the corresponding photoluminescence from wurtzite (WZ) and zinc blende (ZB) crystal phases, respectively. α, β, and γ represent all possible optical transitions. (b) High-resolution transmission electron microscopy image of a single InP nanowire. Blue and red lines are guides to the eye corresponding to atomic planes of wurtzite and zinc blende crystal structures, respectively. (c) Photoluminescence of a single InP nanowire under increasing excitation power.

increasing excitation power the spectral lines broaden and blue shift due to energy states filling in QDs. The WZ line shows no spectral shift. This is expected since under the low excitation rates used here the emission is predominantly governed by ground-state electron−hole recombinations.

Time-resolved photoluminescence measurements are represented in Figure 2. We clearly observe a short lifetime for optical transitions of type α. A monoexponential fit to the experimental data gives a lifetime of 120 ± 7 ps. Emission peaks at lower energies, labeled ZB/WZ, cor-
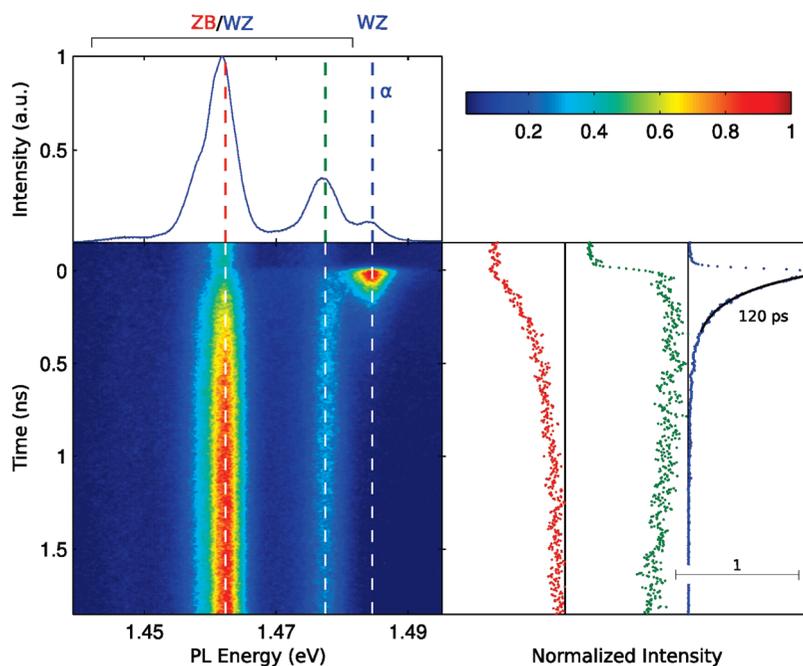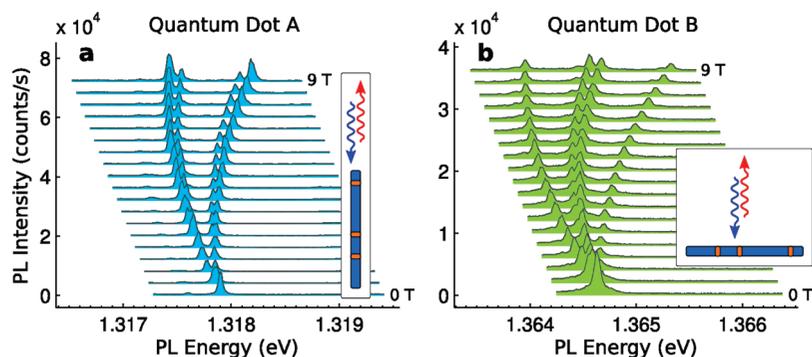

FIGURE 2. Time-resolved photoluminescence of a single nanowire with crystal phase heterostructures. False-color plot represents time evolution of the PL after excitation by a laser pulse impinging at time 0. The upper part represents the PL intensity integrated over the full time window of 2 ns. The time evolutions of the PL peaks correspond to the cuts in the false-color plot, indicated by dashed lines and shown in the graph on the right with the corresponding colors. The black solid line represents a monoexponential fit to the experimental data.
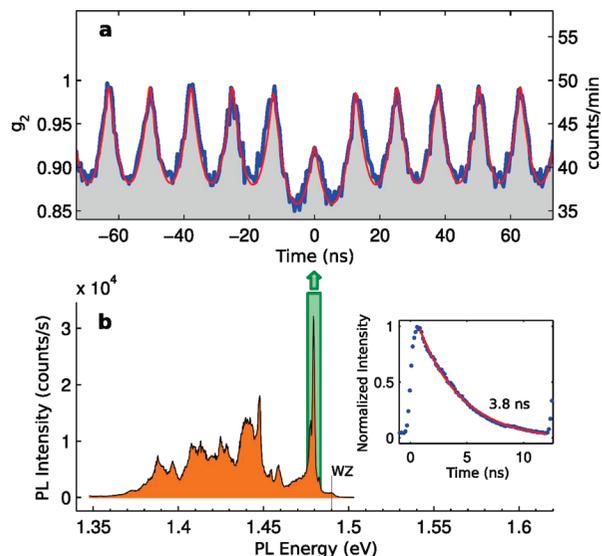
FIGURE 3. Crystal phase quantum dot. (a) Second-order autocorrelation measurement of photons emitted from a few crystal phase QDs under pulsed excitation. The red line is a fit to the model discussed in the text. (b) PL of a single NW. The green area schematically represents a band-pass transmission filter with spectral width of 6 meV. This part was spectrally selected from the rest of the PL for autocorrelation measurements in (a). The inset shows the decay curve measured from a QD emitting at 1.48 eV. The red solid line is a monoexponential fit to the experimental data.

respond to optical transitions of type β or γ. Only a fraction of their decay traces are captured within a 2 ns time window, indicating much longer lifetimes. The data at negative times represent the part of the PL decay curve that was excited by the previous laser pulse 13 ns earlier. A significant signal measured at these times, the tail signal, indicates that electrons and holes can remain in short ZB and WZ sections for more than 13 ns.

Furthermore, the low-energy peak (red decay curve) shows a larger tail signal than the high-energy peak (green decay curve). This means a longer lifetime for the low-energy peak and follows from the NW schematics described in Figure 1a. For example, longer ZB sections will have lower energy levels for electrons. The wave functions of electrons will penetrate less into the WZ region, yielding less overlap with the wave functions of holes resulting in longer lifetimes.

In addition, the decay curve of the low-energy photoluminescence peak (red decay curve) shows longer rise time, compared to the decay curve of high-energy peak (green decay curve). This is because excited electrons have to relax to the lowest energy states in ZB sections before they recombine radiatively. The relaxation process is longer for lower energy states, and therefore, photon emission is delayed, resulting in longer rise times in decay curves.

Long lifetimes, measured in our experiments, lead to another important conclusion—a high purity of the sample. Defects or surface states in a NW that contribute to usually very fast nonradiative decay channels[16] are negligible in these quantum dots.

To demonstrate the quantum nature of crystal phase QDs, we performed photon correlation measurements[15,17] under pulsed excitation, shown in Figure 3a. Missing correlation events at time 0 indicate that the emission originates from a few single photon emitters. From the peak height at time zero, we estimate the number of single photon emitters within the excitation spot to be less than 4. The long lifetimes of electrons and holes in the QD lead to a significant overlap between the neighboring peaks in the correlation measurements, set by the laser repetition rate. For a correct estimation of lifetime we fit with a model with few identical single photon emitters, giving us a lifetime of 5 ± 1 ns.

Figure 3b shows photoluminescence of a single NW, where the green area schematically represents the emission peak spectrally selected for autocorrelation measurements in Figure 3a. The inset shows the lifetime measurements from a QD emitting at 1.48 eV. From a monoexponential fit we obtained a 3.8 ± 0.2 ns lifetime, comparable with 5 ± 1 ns retrieved from the autocorrelation measurements.

To further investigate the physical properties of our QDs, we applied an external magnetic field to the sample. The magneto-photoluminescence measurements of two different QDs in two different experimental configurations are shown in Figure 4. In both QDs we observe a diamagnetic shift and Zeeman splitting.[18] Surprisingly, spectral lines split into four, contrary to only two as is usual in self-assembled QDs.[18] One possible explanation is that an external magnetic field[19] or

FIGURE 4. Magnetic field dependence of crystal phase quantum dots. (a, b) PL of two different crystal phase QDs under application of external magnetic field. The magnetic field is varied from 0 to 9 T with 0.5 T steps. Insets describe the experimental configuration. In both cases the direction of the magnetic field was aligned along the direction of optical excitation end emission.

a strain at WZ–ZB interfaces[20] can mix light and heavy-hole states and allow for additional optical transitions. This is an interesting observation which can be further studied using resonant excitation of QDs and polarization analysis.

To conclude, we have shown formation of crystal phase quantum dots in a homogeneous InP nanowire. This new type of quantum dot independently expresses itself in four different types of experiments: transmission electron microscopy, photoluminescence spectroscopy, lifetime, and photon correlation measurements. Natural charge separation allows for applications like quantum memories[21] and solar cells.[22] These and other applications will also benefit from this clean, defect-free system with sharp monolayer interfaces.

Methods. *Sample.* InP NWs were fabricated by a bottom-up approach based on the vapor–liquid–solid synthesis method implemented with molecular beam epitaxy growth technique on (111)B oriented InP substrates using Au as a catalyst.[23,24] The growth temperature is one of the parameters which influence the crystal phase of the nanowire. A low growth temperature (380 °C) is favorable to pure wurtzite InP while the formation of zinc blende InP sections is highly probable at higher temperature (420 °C). The samples under study were grown with two growth steps at high and low temperatures, successively.

Experimental Setup. Micro-photoluminescence studies were performed at 4.2 K. The NW was excited with 532 nm continuous wave or 780 nm ps pulsed lasers focused to a spot size of 1 μm using a microscope objective with numerical aperture 0.85. The PL signal was collected by the same objective and was sent to a spectrometer, which dispersed the PL onto a nitrogen-cooled silicon array detector or streak camera, enabling 30 μeV spectral and 20 ps temporal resolution. For photon correlation measurements, PL signal was filtered by a grating based filter, enabling 6 meV resolution, and sent trough a fiber beamsplitter into two single photon detectors with 500 ps temporal resolution.

Model. Our model is based on a few identical single photon emitters with lifetime τ. Each peak is a monoexponential decay convoluted with the temporal response of the system. The peak at time 0 was multiplied by a factor N to fit the antibunching dip. τ and N are independent fit parameters.

REFERENCES AND NOTES

(1) Yu, P. Y.; Cardona, M. *Fundamentals of Semiconductors: Physics and Materials Properties*; Springer: Berlin, 2005.

(2) Algra, R. E.; Verheijen, M. A.; Borgstrom, M. T.; Feiner, L. F.; Immink, G.; van Enckevort, W. J. P.; Vlieg, E.; Bakkers, E. P. A. M. *Nature* **2008**, *456*, 369–372.

(3) Caroff, P.; Dick, K. A.; Johansson, J.; Messing, M. E.; Deppert, K.; Samuelson, L. *Nat. Nanotechnol.* **2009**, *4*, 50–55.

(4) Koguchi, M.; Kakibayashi, H.; Yazawa, M.; Hiruma, K.; Katsuyama, T. *Jpn. J. Appl. Phys.* **1992**, *31*, 2061–2065.

(5) Murayama, M.; Nakayama, T. *Phys. Rev. B* **1994**, *49*, 4710–4724.

(6) Duan, X.; Huang, Y.; Cui, Y.; Wang, J.; Lieber, C. M. *Nature* **2001**, *409*, 66–69.

(7) Wagner, R. S.; Ellis, W. C. *Appl. Phys. Lett.* **1964**, *4*, 89–90.

(8) Hiruma, K.; Katsuyama, T.; Ogawa, K.; Koguchi, M.; Kakibayashi, H.; Morgan, G. P. *Appl. Phys. Lett.* **1991**, *59*, 431–433.

(9) Jacobs, B. W.; Ayres, V. M.; Stallcup, R. E.; Hartman, A.; Tupta, M. A.; Baczewski, A. D.; Crimp, M. A.; Halpern, J. B.; He, M.; Shaw, H. C. *Nano Lett.* **2007**, *7*, 1435–1438.

(10) Bao, J.; Bell, D. C.; Capasso, F.; Wagner, J. B.; Martensson, T.; Tradgardh, J.; Samuelson, L. *Nano Lett.* **2008**, *8*, 836–841.

(11) Pemasiri, K.; Montazeri, M.; Gass, R.; Smith, L. M.; Jackson, H. E.; Yarrison-Rice, J.; Paiman, S.; Gao, Q.; Tan, H. H.; Jagadish, C.; Zhang, X.; Zou, J. *Nano Lett.* **2009**, *9*, 648–654.

(12) Hoang, T. B.; Titova, L. V.; Jackson, H. E.; Smith, L. M.; Yarrison-Rice, J. M.; Lensch, J. L.; Lauhon, L. J. *Appl. Phys. Lett.* **2009**, *94*, 133105.

(13) Ikonic, Z.; Srivastava, G. P.; Inkson, J. C. *Phys. Rev. B* **1995**, *52*, 14078–14085.

(14) Dekel, E.; Gershoni, D.; Ehrenfreund, E.; Spektor, D.; Garcia, J. M.; Petroff, P. M. *Phys. Rev. Lett.* **1998**, *80*, 4991–4994.

(15) Michler, P.; Kiraz, A.; Becher, C.; Schoenfeld, W. V.; Petroff, P. M.; Zhang, L.; Hu, E.; Imamoglu, A. *Nature* **2000**, *406*, 968–970.

(16) Mattila, M.; Hakkarainen, T.; Lipsanen, H.; Jiang, H.; Kauppinen, E. I. *Appl. Phys. Lett.* **2007**, *90*, No. 033101.

(17) Hanbury-Brown, R.; Twiss, R. Q. *Nature* **1956**, *177*, 27–29.

(18) Bayer, M.; Ortner, G.; Stern, O.; Kuther, A.; Gorbunov, A. A.; Forchel, A.; Hawrylak, P.; Fafard, S.; Hinzer, K.; Reinecke, T. L.; Walck, S. N.; Reithmaier, J. P.; Klopf, F.; Schafer, F. *Phys. Rev. B* **2002**, *65*, 195315.

(19) Ancilotto, F.; Fasolino, A.; Maan, J. C. *Phys. Rev. B* **1988**, *38*, 1788–1799.

(20) Kumagai, M.; Chuang, S. L.; Ando, H. *Phys. Rev. B* **1998**, *57*, 15303–15314.

(21) Kroutvar, M.; Ducommun, Y.; Heiss, D.; Bichler, M.; Schuh, D.; Abstreiter, G.; Finley, J. J. *Nature* **2004**, *432*, 81–84.

(22) Tian, B.; Zheng, X.; Kempa, T. J.; Fang, Y.; Yu, N.; Yu, G.; Huang, J.; Lieber, C. M. *Nature* **2007**, *449*, 885–889.

(23) Tchernycheva, M.; Cirlin, G. E.; Patriarche, G.; Travers, L.; Zwiller, V.; Perinetti, U.; Harmand, J.-C. *Nano Lett.* **2007**, *7*, 1500–1504.

(24) Glas, F.; Harmand, J. C.; Patriarche, G. *Phys. Rev. Lett.* **2007**, *99*, 146101.